Bioorganic Chemistry 90 (2019) 103075

Contents lists available at ScienceDirect

Bioorganic Chemistry

journal homepage: www.elsevier.com/locate/bioorg

Human neutrophil elastase (HNE) inhibitory polyprenylated acylphloroglucinols from the flowers of *Hypericum ascyron*

Zuo Peng Li, Jeong Yoon Kim, Yeong Jun Ban, Ki Hun Park*

Division of Applied Life Science (BK21 plus), IALS, Gyeongsang National University, Jinju 52828, Republic of Korea

ARTICLE INFO

Keywords:
Hypericum ascyron
Human neutrophil elastase
Polycyclic polyprenylated acylphloroglucinols
Enzyme kinetics

ABSTRACT

In the course of an investigation of human neutrophil elastase (HNE) associated with inflammation, the extract of the flower parts of *Hypericum ascyron* showed a significant influence to HNE. The responsible metabolites to HNE inhibition were found to be eight polyprenylated acylphloroglucinols, PPAPs (**1–8**) which showed IC_{50} ranges between 2.4 and 19.9 μM. This is the first report to demonstrate that PPAP skeleton exhibits potent HNE inhibition. The compounds **1–3** were characterized and newly named as ascyronone E (IC_{50} = 4.3 μM), ascyronone F (IC_{50} = 19.9 μM), ascyronone G (IC_{50} = 4.5 μM) based on 2D-NMR spectroscopic data. In the kinetic analysis of double reciprocal plots, all the compounds showed noncompetitive behaviors to HNE enzyme with the remaining of K_m and the increase of V_{max}. The binding affinity levels (K_{SV}) by using fluorescence were sufficient to be able to prove that PPAPs (**1–8**) had compliant interaction with inhibitory potencies.

1. Introduction

Human neutrophil elastase (HNE, EC 3.4.21.37) belonging to serine protease, is a proteolytic enzyme associated with the response to inflammatory stimuli [1]. HNE is present in azurophilic of neutrophils and regulated under normal condition by endogenous inhibitors such as α1-protein and α-macroglobin [2,3]. The activity of HNE is evaluated upon exposure to oxidative stress, cytokines and chemoattractants such as interleukin (IL)-8, c5a and LPS [4]. The elevated HNE activity associated with inflammatory disorders such as chronic obstructive pulmonary disease (COPD), atherosclerosis, psoriasis, and dermatitis [5]. Thus a number of clinical observations demonstrated that HNE enzyme represents a good therapeutic target for the treatment of inflammatory disease.

Hypericum ascyron belongs to the Guttiferae family and is widely distributed in eastern Asia. It has been used as a traditional Chinese medicine for treatment for headache, rheumatism, and abscesses [6]. This plant is well-known for the source of unique and complex polycyclic polyprenylated acylphloroglucinols (PPAPs) [7]. PPAPs have been applied to various biological targets, such as antidepressants, anti-inflammatory, antiviral, antibacterial, anti-tumor, anti-neurodegenerative, and anti-HIV activities [8–11]. Thus the major biological functions concerned with inflammation which are deeply associated with HNE inhibition.

The present study aimed to investigate the metabolites in *Hypericum ascyron* targeting to HNE inhibition. All isolated compounds were examined for their HNE inhibitory activities, followed by an investigation of their inhibitory mechanism and binding affinities.

2. Materials and methods

2.1. General experimental procedures

1D and 2D NMR spectra were recorded on a Bruker (AM 500 MHz) spectrometer (Billerica, MA), using either $CDCl_3$ or acetone-D_6 as solvent and tetramethylsilane (TMS) as an internal standard. Infrared (IR) spectra were recorded on a Varian 640-IR (Varian, Inc. USA) infrared Fourier transform spectrophotometer (KBr). UV spectra were measured using a Beckman DU650 spectrophotometer. Electron ionization (EI) and EI high-resolution (HR) mass spectra were obtained on a JEOL JMS-700 instrument (JEOL, Tokyo, Japan). A UPLC system coupled with Q-TOF/MS (from Waters Corp. Milford, MA, USA) was used for ESIMS and HRESIMS analysis. Optical rotations were measured on a Perkin-Elmer 343 polarimeter (Perkin-Elmer, Bridgeport, USA). Column chromatography was performed using silica gel (230–400 mesh; Merck Co., Darmstadt, Germany), YMC-gel ODS-A (S-75 μm; YMC), and Sephadex LH-20 (GE Healthcare Bio-science AB, Uppsala, Sweden). MPLC was conducted on a Forte/R 100 (YMC Co., Ltd., Kyoto, Japan) and recycle HPLC conducted on a LC-9130G NEXT (JAI Co., Ltd., Tokyo, Japan). Enzymatic assays were carried out on a SpectraMax M3 Multi-Mode microplate reader (Molecular Devices, USA). All chemicals were analytical grade.

* Corresponding author.
E-mail address: khpark@gnu.ac.kr (K.H. Park).

https://doi.org/10.1016/j.bioorg.2019.103075
Received 27 April 2019; Received in revised form 12 June 2019; Accepted 17 June 2019
Available online 20 June 2019

2.2. Plant material

Flowers were collected at Gyeongsang National University, Jinju, Gyeongsangnam-do, Korea, in June 2017 and identified by Prof. Jae Hong Park. A voucher specimen (KHPark 082517) of this raw material is deposited at the Herbarium of Kyungpook National University.

2.3. Extraction and isolation

Dried flowers of *H. ascyron* (5.5 kg) were extracted with methanol (15 L × 3) at room temperature to obtain the extract (360 g). The extracted residue was suspended in H_2O (1 L) and further partitioned with hexane (3 L × 3) to give the hexane extract (65 g). The hexane extract was subjected to silica gel column (15 × 30 cm, 230–400 mesh, 600 g) with elution using a gradient of increasing ethylacetate (2–50%) in hexane to give eight fractions (A-H). Herein, the fractions D and E were selected for further purification because of their HNE inhibitory potential. Fraction D (4.5 g) was subjected to silica gel column (5 × 30 cm, 300 g) using a gradient of increasing ethylacetate (2–50%) in hexane to give four fractions (D1-D4). Fraction D2 (809 mg) was fractionated via MPLC using C18 column (25 × 300 mm, 50 μm, 130 g) with elution using a gradient of increasing MeOH (40–100%) in H_2O to afford four major fractions (D2a-2d). D2b (86.5 mg) was purified by recycling HPLC with C18 (20 × 250 mm, 10 μm, 100 Å) eluting with 90% MeOH in H_2O to afford compounds **1** (16.2 mg) and **5** (12.6 mg). D2c (39.6 mg) provided compounds **2** (16.2 mg) and **6** (14.0 mg) under the same recycling HPLC condition. D2d (32.5 mg) gave compounds **7** (9.2 mg) and **8** (11.2 mg) by the same recycling HPLC condition. Fraction E (8.2 g) was subjected to a silica gel column with elution using a gradient of increasing ethylacetate (2–50%) to give five fractions (E1-E5). Fraction E2 (600 mg) was fractionated via MPLC using C18 column (25 × 300 mm, 50 μm, 130 g) to give four fractions (E2a-E2d). The fraction E2c (108 mg) was more chromatographed by recycling HPLC with C18 (20 × 250 mm, 10 μm, 100 Å) eluting with 90% MeOH in H_2O to afford compounds **3** (32.0 mg) and **4** (12.1 mg).

Ascyronone E (**1**): colorless oil; $[\alpha]_D^{20}$ – 86.8 (*c* 0.1, MeOH); UV (MeOH) λ_{max} (log ε) 205 (4.15), 242 (4.06), 336 (4.00) nm; IR (KBr) ν_{max} 3421, 2973, 2932, 1752, 1590 cm^{-1}; ^1H and ^{13}C NMR data, see Table 1; HRESIMS: *m/z* 569.3676, $[M-H]^+$ (calcd. for $C_{38}H_{50}O_4$, 569.3670).

Ascyronone F (**2**): colorless oil; $[\alpha]_D^{20}$ + 36.5 (*c* 0.1, MeOH); UV (MeOH) λ_{max} (log ε) 205 (4.18), 230 (4.27), 251 (4.11) nm; IR (KBr) ν_{max} 3437, 2973, 2932, 1731, 1625 cm^{-1}; ^1H and ^{13}C NMR data, see Table 1; HREIMS: *m/z* 586.3650, $[M]^+$ (calcd. for $C_{38}H_{50}O_5$, 586.3658).

Ascyronone G (**3**): colorless oil; $[\alpha]_D^{20}$ + 69.6 (*c* 0.1, MeOH); UV (MeOH) λ_{max} (log ε) 205 (4.11), 230 (4.18), 270 (4.09) nm; IR (KBr) ν_{max} 3422, 2932, 2852, 1715, 1630 cm^{-1}; ^1H and ^{13}C NMR data, see Table 1; HREIMS: *m/z* 518.3034, $[M]^+$ (calcd. for $C_{33}H_{42}O_5$, 518.3034).

Table 1
^1H and ^{13}C NMR of new compounds (**1–3**) in $CDCl_3$.

Position	**1**		**2**		**3**	
	δ_C	δ_H (*J*, Hz)	δ_C	δ_H (*J*, Hz)	δ_C	δ_H (*J*, Hz)
1	68.4		70.6		55.2	
2	210.8		206.8		178.1	
3	62.0		65.0		110.0	
4	40.1	1.97, 1.47, m	190.4		186.9	
5	51.6	1.61, m	171.5		107.9	
6	51.1		118.9		195.1	
7	83.3		49.9		194.4	
8	109.5		41.4	1.80, m	138.3	
9	198.4		40.9	2.01, 1.44, m	127.7	7.37, m
10	52.5	1.74, m	193.2		127.8	7.43, m
11	14.0	1.09, s	137.7		131.0	7.45, m
12	174.4		128.5	7.56, d (10.0)	127.8	7.43, m
13	135.0		128.2	7.34, dd (10.0, 9.5)	127.7	7.37, m
14	127.9	7.47, m	132.7	7.49, t (9.5)	26.8	3.04, dd (15.2, 10.7) 2.97, dd (15.2, 6.9)
15	128.0	7.44, m	128.2	7.34, dd (10.0, 9.5)	92.6	4.72, dd (10.7, 6.9)
16	130.4	7.47, m	128.5	7.56, d (10.0)	71.6	
17	128.0	7.44, m	37.9	1.69, m	23.8	1.21, s
18	127.9	7.47, m	25.9	2.09, m	26.3	1.32, s
19	23.2	2.59, m	124.4	5.05, m	37.4	2.49, 2.68, m
20	119.2	5.02, m	131.9		119.4	4.88, m
21	133.5		25.6	1.66, s	135.0	
22	18.1	1.71, s	17.7	1.58, s	18.1	1.62
23	17.9	1.66, s	14.8	1.27, s	25.7	1.64
24	29.6	2.14, 2.41, m	28.3	2.11, m	37.3	2.52, 2.62, m
25	120.1	4.97, m	122.1	5.02, m	117.7	4.98, m
26	133.5		133.5		139.2	
27	17.9	1.50, s	25.7	1.69, s	16.2	1.60, s
28	26.1	1.63, s	18.0	1.57, s	39.8	1.94, m
29	32.9	1.88, 2.13, m	29.5	2.49, 2.58, m	26.6	1.96, m
30	123.3	4.95, m	119.5	5.02, m	123.8	5.03, m
31	131.8		134.7		131.8	
32	25.7	1.65, s	18.1	1.69, s	17.6	1.56, s
33	18.0	1.55, s	26.0	1.68, s	25.7	1.65, s
34	26.2	1.92, m	26.3	2.95, dd (10.0, 4.8)		
35	124.8	4.89, m	93.4	4.61, dd (10.0, 4.8)		
36	131.5		70.5			
37	25.7	1.57, s	23.8	0.92, s		
38	26.0	1.66, s	26.5	0.87, s		
12-OH		15.4				

2.4. Measurement of neutrophil elastase activity

HNE (EC 3.4.21.37) activity was assayed using standard procedures with slight modifications by measuring the formation of *p*-nitroaniline after *N*-methoxysuccinyl-Ala-Ala-Pro-Val-*p*-nitro anilide hydrolysis at 405 nm [12]. Test samples were dissolved in dimethyl sulfoxide (DMSO) at a stock concentration of 10 mM and used for the assay after diluting. The reaction mixture contained 130 μL 0.02 mM Tris-HCl buffer (pH 8.0), 10 μL test sample solution, 40 μL substrate (1.5 mM, MeOSuc-AAPV-*p*NA), and 20 μL human neutrophil elastase (0.2 units/mL) and was placed in 96-well microplates. The reaction mixtures were mixed and incubated for 15 min at room temperature and then screened at 405 nm for 30 min every 30 *sec*. Inhibitory activities were further characterized by determining the concentration required to inhibit 50% of the enzyme activity (IC_{50}), which was calculated using the following equation: Activity (%) = 100 [1/(1 + ([I]/IC_{50}))], where [I] is the concentration of inhibitor.

2.5. Fluorescence quenching measurements

All fluorescence spectra were measured on a SpectraMax M3 multimode microplate reader (Molecular Devices, CA, USA) equipped with a thermostat bath using 96-well immuno-plates (SPL, Life Sciences, Korea). For a typical measurement of fluorescence, 180 μL 0.02 mM Tris-HCl buffer with 10 μL of 0.01 unit/mL neutrophil elastase was accurately added to the 96 wells; different concentrations of inhibitor (10 μL) were then added. The automatic shaking feature of the microplate reader was utilized to shake the reaction solutions. Spectra for the fluorescent emissions were recorded at 18 °C and 37 °C, with the width of the excitation and emission slits adjusted to 2.0 nm. The excitation wavelength was 260 nm, and the emission spectra were recorded from

280 to 400 nm [13]. We analyzed the Stern-Volmer quenching constant (K_{SV}) using Eq. (1). All experiments were conducted in triplicate, and the mean values were calculated.

$$F_0 - F = 1 + K_{SV}[Q] \quad (1)$$

2.6. Statistical analysis

All experiments were conducted in triplicate. Results were analyzed using variance analysis with Sigma Plot (version 10.0, Systat Software, Inc., San Jose, CA). Differences were considered significant at $p < 0.05$.

3. Results and discussion

3.1. Characterization of the isolated compounds

The higher potency and dose-dependent human neutrophil elastase (HNE) inhibitory activity of the methanol extract of *H. ascyron* flowers (IC_{50} = 115 μg/ml) encouraged us to identify the responsible compounds. Eight compounds (**1**–**8**, shown in Fig. 1) were identified as polyprenylated acylphloroglucinols by means of detailed spectroscopic data (supplementary data) and comparing the results with previously reported data. The isolated compounds were ascyronone E (**1**), ascyronone F (**2**), ascyronone G (**3**), hypelodin B (**4**) [14], hypercohin K (**5**) [15], furohyperforin (**6**) [16], hypercohin G (**7**) [17], and hyphenrone X (**8**) [18]. The compounds (**1**–**3**) emerged as new polyprenylated acylphloroglucinol derivatives.

Ascyronone E (**1**) was obtained as a colorless oil {$[\alpha]_D^{20}$ – 86.8 (*c* 0.1, MeOH)} possessing a molecular formula $C_{38}H_{50}O_4$ and 14 degrees of unsaturation, as established by HRESIMS, (*m/z* 569.3676 $[M-H]^-$, calcd 569.3670). The IR spectrum displayed absorption bands due to hydroxyl (3433 cm^{-1}) and carbonyls groups (1752 cm^{-1}). Comprehensive analysis of NMR data (Table 1), two carbonyl groups (δ_C 210.8 for *C*2, δ_C 198.4 for C9), two α-position carbons (δ_C 62.0 for C3, δ_C 68.4 for C1), enolic carbon C8 (δ_C 109.5), and oxygenated carbon C7 (δ_C 83.3) revealed that compound **1** is tricyclo [4.3.1.$0^{3,7}$] decane derivative similar to that of nemorosonol as isolated from *Clusia nemorosa* [19]. Four prenyl groups were proved by successive proton cross peaks as follow: H19/H20/H22, H24/H25/H27, H29/H30/H32, and H34/H35/H37, respectively. The positions of four prenyl groups at C1, C3, C5 and C10 were confirmed by HMBC correlations from H19 to C1 (δ_C 68.4), C2 (δ_C 210.8), and C10 (δ_C 52.5), and from H24 to C2, C3, and C4, and from H29 to C4 (δ_C 40.1), C5 (δ_C 51.6), and C6 (δ_C 51.1), and form H34 to C1 (δ_C 68.4), C6 (δ_C 51.1), and C10 (δ_C 52.5), respectively (Fig. 2). The position of enolic carbon C12 was confirmed by HMBC correlations from enolic OH (δ_H 15.4) to C8 (δ_C 109.5), C12 (δ_C 174.4) and C13 (δ_C 135.0). The relative stereochemistry of **1** was confirmed by NOESY experiment (Fig. 3). The successive NOE cross peaks between H29, H11 and H34 revealed that prenyl at C5, methyl at C6 and prenyl at C10 are in the same direction. The prenyl at C3 is on the same side with the benzoyl group at C8 because of NOE cross peak

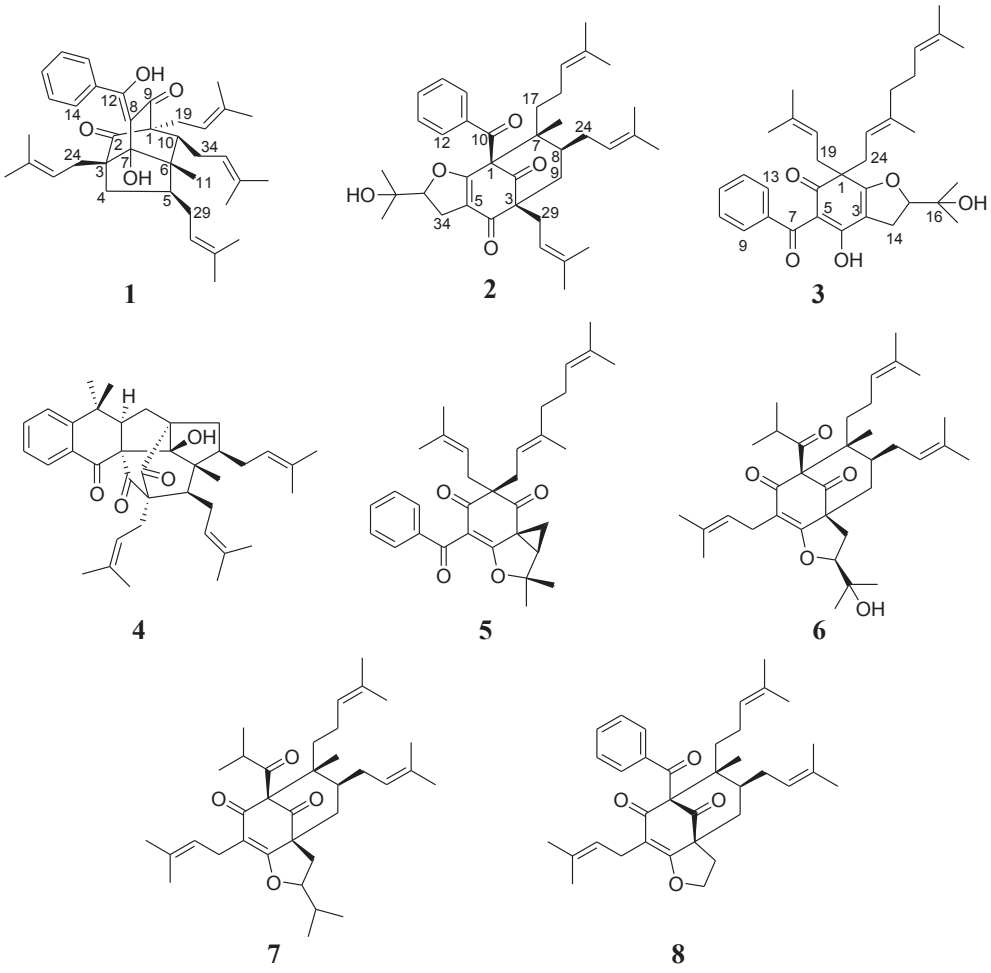

Fig. 1. Chemical structures of isolated compounds **1**–**8** from *Hypericum ascyron*.

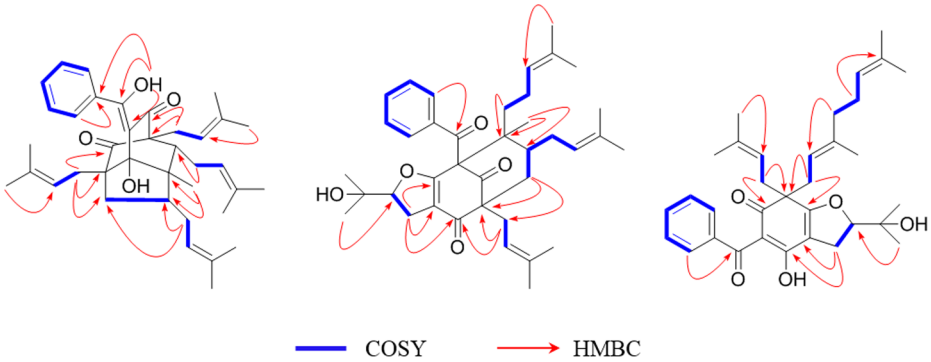

Fig. 2. Key ^{1}H–^{1}H COSY and HMBC correlations of compounds **1**–**3**.

between H24 and H15. It is a natural result that methyl at C6 and prenyl at C3 must exist in the same direction, when we consider the uniqueness of tricycle [4.3.1.$0^{3,7}$] decane structure. This molecule showed the unique cotton effects in the electronic circular dichroism (ECD) spectrum (Supplementary material, Fig. S11). Thus the structure of **1** was determined ascyronone E with tricycle [4.3.1.$0^{3,7}$] decane core.

Ascyronone F (**2**) was a colorless oil {$[\alpha]_D^{20}$ + 36.5 (*c* 0.1, MeOH)}, possessing a molecular formula $C_{38}H_{50}O_5$ by $[M]^+$ ion at 586.3650 (calcd 586.3658) in the HREIMS. The IR spectrum displayed absorption bands due to hydroxyl (3422 cm^{-1}) and carbonyls groups (1715 cm^{-1}) Three carbonyl carbons (δ_C 206.8 for *C*2, δ_C 190.4 for C4, δ_C 193.2 for C10), enolic carbon (C5, δ_C 171.5) and two α-position carbons (δ_C 70.6 for C1, δ_C 65.0 for C3) indicated a tetraketone motif for **2**, which agreed with hyperascyrin E [20]. The methylpentenyl group at C7 was revealed by successive proton cross peaks from H17 to H22, and its location was confirmed by HMBC correlations from H17 to C7 (δ_c 49.9) and C23 (δ_c 14.8). Two prenyl groups at C3 and C8 were confirmed by successive proton cross peaks of H24/H25/H27 and H29/H30/H32, respectively. Their positions were proved by HMBC correlations from H24 to C8 (δ_c 41.4), C7 (δ_c 49.9), and from H29 to C3 (δ_c 65.0) C4 (δ_c 190.4), respectively (Fig. 2). The dihydrofuran motif was confirmed by the coupling between H34 (δ_H 2.95, dd) and H35 (δ_H 4.61, dd), and HMBC correlations from the oxygenated proton H35 (δ_H 4.61) to C34 (δ_c 26.3) and C36 (δ_c 70.5). The relative stereochemistry of **2** was confirmed by NOESY experiment. The methyl at C7 and prenyl at C8 were oriented in the same direction because of a strong NOE cross peak between H23 and H24. The NOE cross peak between H12 and H30 was proved to be the same direction of benzoyl at C1 with prenyl at C32. The ECD spectrum of 2 was illustrated at supplementary material (Fig. S23). Thus the structure of **2** was determined ascyronone F with bicycle [3.3.1] nonane core.

Ascyronone G (**3**) was isolated as colorless oil {$[\alpha]_D^{20}$ + 69.6 (*c* 0.1, MeOH)}, possessing a molecular formula $C_{33}H_{42}O_5$ by the $[M]^+$ ion at 518.3034 (calcd 518.3034) in HREIMS. The ^{1}H NMR signals (δ_H 7.37, 2H; 7.43, 2H; 7.45, 1H) indicated the presence of a benzoyl group. Three carbonyl signals (δ_C 195.1, 186.9, 178.1) and lower chemical shift of α-position carbon 5 (δ_C 107.9) proposed the presence of β-triketone motif. The presence of prenyl and geranyl groups was proved by successive cross peaks from H19 to H22, and from H24 to H32. The prenyl and geranyl at the same carbon C1 (δ_C 55.2) were confirmed by that both H19 (δ_H 2.49, 2.68) and H24 (δ_H 2.52, 2.62) signals had the same HMBC correlations with C1 (δ_C 55.2), C6 (δ_C 195.1), and C2 (δ_C 178.1) (Fig. 2). The presence of dihydrofuran motif was deduced from proton coupling between H14 and H15, and HMBC correlations from oxygenated H15 (δ_H 4.72) to C14 (δ_C 26.8) and C16 (δ_C 71.6). Thus, the structure of **3** was determined as ascyronone G with β-triketone motif.

3.2. HNE inhibition of the isolated compounds

The HNE activity was measured in the presence and absence of the tested compounds using a chromogenic assay [21]. The tested compounds (**1**–**8**) exhibited a significant dose dependent inhibition against HNE with IC_{50} values in the range of 2.4–19.9 μM (Table 2). The most potent inhibitor was found to be furohyperforin (**6**) with 2.4 μM of IC_{50}. However, HNE inhibitory activity was slightly affected by subtle

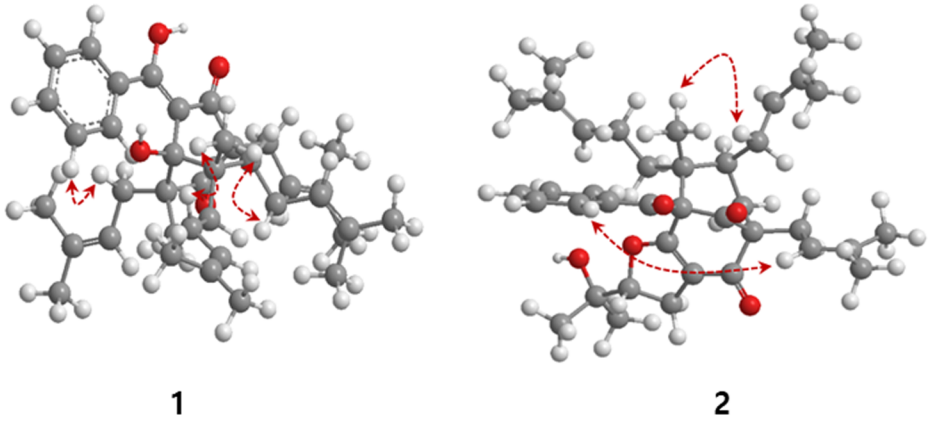

Fig. 3. Key NOESY correlations of compounds **1** and **2**.

Table 2
Inhibitory effects of compounds (**1**–**8**) on HNE activities.

Compounds	IC_{50} (μM)[a]	Type of inhibition (K_i[b], μM)
1	4.3 ± 0.4	Non-competitive (4.1 ± 0.2)
2	19.9 ± 0.1	Non-competitive (18.2 ± 0.3)
3	4.5 ± 0.2	Non-competitive (3.9 ± 0.1)
4	15.5 ± 1.2	Non-competitive (14.6 ± 0.5)
5	9.4 ± 0.6	Non-competitive (8.5 ± 0.4)
6	2.4 ± 0.3	Non-competitive (1.8 ± 0.4)
7	4.9 ± 0.2	Non-competitive (4.3 ± 0.1)
8	5.8 ± 0.5	Non-competitive (4.9 ± 0.6)
Caffeic acid[d]	67.7 ± 0.9	NT[c]

[a] All compounds were examined as set of experiments repeated three times; IC_{50} values of compounds represent the concentration that caused 50% enzyme activity loss.
[b] Values of inhibition constant.
[c] NT: not tested
[d] Positive control.

changes in the respective structures of compounds. Isobutanoyl at C1 displayed 8-folds effective than benzoyl derivatives such as **6** (IC_{50} = 2.4 μM) *vs* **2** (IC_{50} = 19.9 μM). The hydroxyl group of dihydrofuran motif affected to increase 2-folds inhibitory potency in comparison of **6** and **7** (IC_{50} = 4.9 μM).

Kinetic analysis of the inhibitors, all of the compounds (**1**–**8**) displayed the same between enzyme activity and enzyme concentration to be reversible inhibitors. All compounds showed dose-dependent inhibition to HNE enzyme as like compound **1** (Fig. 4A). Fig. 4B is the plot of the initial velocity versus enzyme concentration in the presence of a different concentration of representative inhibitor **1** (IC_{50} = 4.3 μM). Increasing the concentration of inhibitor resulted in lowering of the slope lines, which pass through the origin. It indicated that compound **1** was a reversible inhibitor. The HNE enzyme inhibitory behaviors of compounds (**1**–**8**) were modeled using double-reciprocal plots. In Lineweaver-Burk plot analysis, the increasing concentration of **1** led V_{max} decrease without changing K_m value. As the graph can be seen clearly, $-1/K_m$ (the x-intercept) was not affected by concentrations, while $-1/V_{max}$ (the y-intercept) became more positive. Thus compound **1** had noncompetitive inhibition characteristics for HNE (Fig. 4C). The K_i value of inhibitor **1** was estimated as 4.1 μM by Dixon plots (Fig. 4D).

For enzyme inhibition, the inhibitor binds first to the enzyme and then blocks its function. Thus it might be necessary to examine a binding affinity together with inhibitory potency to prove an inhibitory function clearly. The intrinsic fluorescence of protein from tryptophan (Trp), tyrosine (Tyr), and phenylalanine (Phe) changes as a function of ligand concentrations. Trp residue is the most sensitive residue [22]. Human neutrophil elastase has three most fluorogenic Trp residues including Trp-12, Trp-127, and Trp-212. The enzyme binding affinities of inhibitors were investigated by the quenching fluorescence spectra [13]. As shown in Fig. 5, the fluorescence intensities were decreased by inhibitor concentrations and inhibitory potencies. Fig. 5A and B showed that compound **1** (IC_{50} = 4.3 μM) decreased the fluorescence intensity significantly by concentrations between 7.8 ~ 31.2 μM, whereas the less effective compound **2** (IC_{50} = 19.9 μM) was not affected to FQ at the same concentration. The FQ effects of the remaining compounds were displayed in supplementary materials (Table S1). The binding affinity level (K_{SV}) was analyzed using the Stern-Volmer Eq. (1). The binding affinities (K_{SV}) are in agreement with their inhibitory potencies (Table 2 and Fig. 5C).

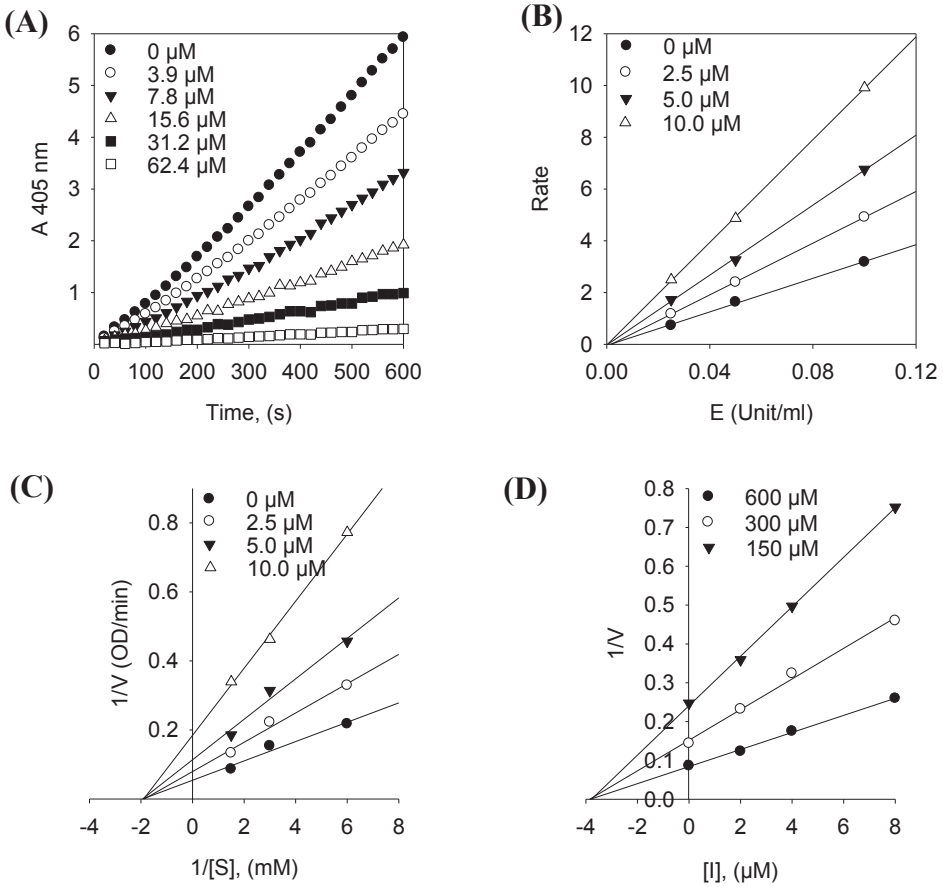

Fig. 4. (A) Dose-dependent inhibitory effects of isolated compound **1** on HNE. (B) Determination of the reversible inhibitory mechanism of compound **1**. (C) Lineweaver-Burk plot for HNE inhibition by compound **1**. (D) Dixon plot for HNE inhibition by compound **1**.

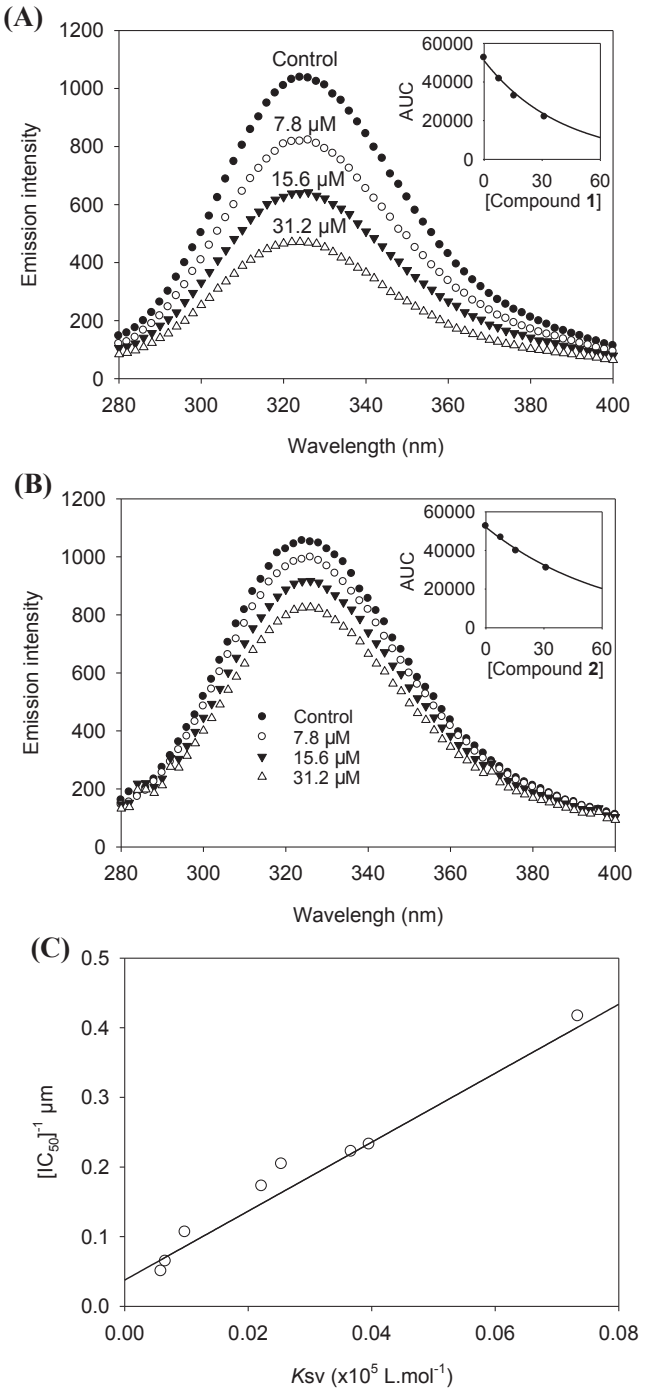

Fig. 5. The fluorescence emission spectra (A and B) of neutrophil elastase (NE) at different concentration of compounds **1** and **2** (Inset) Normalized intensities of fluorescence for NE are shown for compounds **1** and **2**, respectively. (C) The correlation between half maximal inhibitory concentration (IC_{50}) values and Stern-Volmer constants (*K*sv) of compounds **1–8** is shown.

4. Conclusions

In conclusion, we have undertaken a thorough investigation of HNE inhibition by the flowers of *H. ascyron*. The principal components were identified as eight PPAPs derivatives, including three new compounds ascyronone E, ascyronone F, and ascyronone G. They showed non-competitive behavior toward HNE. The binding affinity levels (K_{SV}) were sufficient to be able to prove that PPAPs had compliant interaction with inhibitory potency. Finding the results of HNE inhibition would contribute to further inflammation study of PPAPs or *H. ascyron*.

Declaration of Competing Interest

The authors report no conflicts of interest.

Acknowledgements

This work was done with research funds from the National Research Foundation of Korea (NRF, 2018R1A2B6001753) and the Next-Generation BioGreen 21 program, Rural Development Administration (SSAC, No. PJ01318601), Republic of Korea. The BK21 Plus program supported scholarships for all students.

Appendix A. Supplementary material

Supplementary data to this article can be found online at https://doi.org/10.1016/j.bioorg.2019.103075.

References

[1] L. Crocetti, I.A. Schepetkin, A. Cilibrizzi, A. Graziano, C. Vergelli, D. Giomi, A.I. Khlebnikov, M.T. Quinn, M.P. Giovannoni, Optimization of N-benzoylindazole derivatives as inhibitors of human neutrophil elastase, J. Med. Chem. 56 (2013) 6259–6272, https://doi.org/10.1021/jm400742j.
[2] K.M. Heutinck, I.J.M. ten Berge, C.E. Hack, J. Hamann, A.T. Rowshani, Serine proteases of the human immune system in health and disease, Mol. Immunol. 47 (2010) 1943–1955, https://doi.org/10.1016/j.molimm.2010.04.020.
[3] P.A. Henriksen, The potential of neutrophil elastase inhibitors as anti-inflammatory therapies, Curr. Opin. Hematol. 21 (2014) 23–28 doi:10.1097/MOH.0000000000000001..
[4] M. Gorrini, A. Lupi, S. Viglio, F. Pamparana, G. Cetta, P. Iadarola, J.C. Powers, M. Luisetti, Inhibition of human neutrophil elastase by erythromycin and flurythromycin, two macrolide antibiotics, Am. J. Respir. Cell Mol. Biol. 25 (2001) 492–499, https://doi.org/10.1165/ajrcmb.25.4.4552.
[5] P.J. Barnes, R.A. Stockley, COPD: Current therapeutic interventions and future approaches, Eur. Respir. J. 25 (2005) 1084–1106, https://doi.org/10.1183/09031936.05.00139104.
[6] R. Ciochina, R.B. Grossman, Polycyclic polyprenylated acylphloroglucinols, Chem. Rev. 106 (2006) 3963–3986, https://doi.org/10.1021/cr0500582.
[7] X.W. Yang, R.B. Grossman, G. Xu, Research progress of polycyclic polyprenylated acylphloroglucinols, Chem. Rev. 118 (2018) 3508–3558, https://doi.org/10.1021/acs.chemrev. 7b00551.
[8] L. Verotta, Are acylphloroglucinols lead structures for the treatment of degenerative diseases? Phytochem. Rev. 1 (2002) 389–407, https://doi.org/10.1023/A:1026069624278.
[9] B.I.P. Schiavone, A. Rosato, M. Marilena, S. Gibbons, E. Bombardelli, L. Verotta, C. Franchini, F. Corbo, Biological evaluation of hyperforin and its hydrogenated analogue on bacterial growth and biofilm production, J. Nat. Prod. 76 (2013) 1819–1823, https://doi.org/10.1021/np400394c.
[10] N. Huang, L. Rizshsky, C. Hauck, B.J. Nikolau, P.A. Murphy, D.F. Birt, Identification of anti-inflammatory constituents in Hypericum perforatum and Hypericum gentianoides extracts using RAW 264.7 mouse macrophages, Phytochemistry 72 (2011) 2015–2023, https://doi.org/10.1016/j.phytochem.2011.07.016.
[11] D. Li, H. Zhu, C. Qi, Y. Xue, G. Yao, Z. Luo, J. Wang, J. Zhang, G. Du, Y. Zhang, Two new adamantyl-like polyprenylated acylphloroglucinols from Hypericum attenuatum choisy, Tetrahedron Lett. 56 (2015) 1953–1955, https://doi.org/10.1016/j.tetlet.2015.02.056.
[12] Z. Uddin, Z. Li, Y.H. Song, J.Y. Kim, K.H. Park, Visconata: A rare flavonol having long chain fatty acid from Dodonaea viscosa which inhibits Human neutrophil elastase (HNE), Tetrahedron Lett. 58 (2017) 2507–2511, https://doi.org/10.1016/j.tetlet.2017.05.059.
[13] D. Kim, J. Park, J. Kim, C. Han, J. Yoon, N. Kim, J. Seo, C. Lee, Flavonoids as mushroom tyrosinase inhibitors: A fluorescence quenching study, J. Agric. Food Chem. 54 (2006) 935–941, https://doi.org/10.1021/jf0521855.
[14] C. Hashida, N. Tanaka, K. Kawazoe, K. Murakami, H.D. Sun, Y. Takaishi, Y. Kashiwada, Hypelodins A and B, polyprenylated benzophenones from Hypericum elodeoides, J. Nat. Med. 68 (2014) 737–742, https://doi.org/10.1007/s11418-014-0853-9.
[15] X.W. Yang, J. Yang, Y. Liao, Y. Ye, Y.P. Li, S.Y. Yang, F. Xia, G. Xu, Hypercohin K, a polycyclic polyprenylated acylphloroglucinol with an unusual spiro-fused cyclopropane ring from Hypericum cohaerens, Tetrahedron Lett. 56 (2015) 5537–5540, https://doi.org/10.1016/j.tetlet.2015.08.033.
[16] L. Verotta, G. Appendino, E. Belloro, J. Jakupovic, E. Bombardelli, Furohyperforin a prenylated phloroglucinol from St. John's wort (Hypericum perforatum), J. Nat. Prod. 62 (1999) 770–772, https://doi.org/10.1021/np980470v.
[17] X. Liu, X.W. Yang, C.Q. Chen, C.Y. Wu, J.J. Zhang, J.Z. Ma, H. Wang, L.X. Yang, G. Xu, Bioactive polyprenylated acylphloroglucinol derivatives from hypericum cohaerens, J. Nat. Prod. 76 (2013) 1612–1618, https://doi.org/10.1021/np400287r.
[18] Y. Liao, S.Y. Yang, X.N. Li, X.W. Yang, G. Xu, Polyprenylated acylphloroglucinols

from the fruits of Hypericum henryi, Sci. China Chem. 59 (2016) 1216–1223, https://doi.org/10.1007/s11426-016-0052-4.
[19] F.D. Monache, G.D. Monache, R. Moura Pinheiro, L. Radics, Nemorosonol a derivative of tricyclo-[4.3.1.03,7]-Decane-7-hydroxy-2,9-dione from Clusia nemorosa, Phytochemistry 27 (1988) 2305–2308, https://doi.org/10.1016/0031-9422(88)80148-1.
[20] J.W. Hu, M.J. Shi, J.J. Wang, L. Li, J.D. Jiang, T.F. Ji, Methylated polycyclic polyprenylated acylphloroglucinol derivatives from hypericum ascyron, J. Nat. Prod. 81 (2018) 2348–2356, https://doi.org/10.1021/acs.jnatprod.8b00176.
[21] J.Y. Kim, Y. Wang, Z. Uddin, Y.H. Song, Z.P. Li, J. Jenis, K.H. Park, Competitive neutrophil elastase inhibitory isoflavones from the roots of Flemingia philippinensis, Bioorg. Chem. 78 (2018) 249–257, https://doi.org/10.1016/j.bioorg.2018.03.024.
[22] E.A. Burstein, N.S. Vedenkina, M.N. Ivkova, Fluorescence and the location of tryptophan residues in protein molecules, Photochem. Photobiol. 18 (1973) 263–279, https://doi.org/10.1111/j.1751-1097.1973.tb06422.x.